Applied Physics B (2020) 126:72
https://doi.org/10.1007/s00340-020-07420-9

Applied Physics B
Lasers and Optics

Cryogenically cooled, Ho:YAG, Q-switched laser

Miftar Ganija[1,2] · Alexander Hemming[2] · Nikita Simakov[2] · Keiron Boyd[2] · Neil Carmody[2] · Peter Veitch[1] · John Haub[2] · Jesper Munch[1]

Received: 17 December 2019 / Accepted: 16 March 2020 / Published online: 1 April 2020
© Crown 2020

Abstract
The authors report on the performance and scalability of a Q-switched, cryogenically cooled Ho:YAG laser. The Ho:YAG slab was resonantly pumped using a continuous wave thulium fibre laser, and the output energy from the oscillator was extracted using a confocal resonator with a single-pass pump geometry, resulting in 135 mJ at 200 Hz with a beam quality of $M^2 < 1.14$ and a slope efficiency of 66%. A maximum output energy of 165 mJ at 200 Hz was achieved. This first demonstration of a Q-switched cryogenically cooled Ho:YAG laser at high repetition rates shows great potential for further power and energy scaling.

1 Introduction

High-pulse-energy laser sources operating at wavelengths near 2 µm are required for a variety of applications, such as LIDAR, materials processing, spectroscopy, medical and pump sources for high-energy, mid-IR, non-linear frequency conversion. In particular, optical parametric oscillators based on zinc germanium phosphide (ZGP) and cadmium silicon phosphide (CSP) are demonstrated routes to mid-IR generation [1–9]. However, for efficiency and for low risk from optical damage, such non-linear conversion requires a high-energy pump source with a wavelength above 2.05 µm, a large spot size and near diffraction limited beam quality. Such a pump would lead to higher conversion efficiencies and enhanced power scaling opportunities.

The commonly used laser materials in this wavelength regime use holmium as the active ion. However, materials, such as Ho:YLF and Ho:YAG, are quasi three-level at room temperature. As a result, these sources require high pump intensities even to reach transparency. This leads to small pump volumes and mode areas limiting the maximum pulse energies attainable. Attempting to power scale with large mode sizes at room temperature requires prohibitively large pump powers which lead to optical distortions and poor beam quality [1, 10, 11].

The lack of direct pump sources at 1.9 µm led to early attempts to build Q-switched lasers around 2 µm in co-doped architectures using thulium, holmium with flashlamp pumping, resulting in highly multimode laser outputs and poor slope efficiencies [12–14]. Subsequently, different pumping schemes have been exploited for Ho^{3+} materials, including laser diodes, Tm:YLF lasers and Tm:fibre lasers, operating at around 1.9 µm [1–5, 3, 4]. Room-temperature energy scaling of Ho^{3+} in YLF and YAG has been reported by multiple amplifier stages [17–19], whereas oscillator configurations with diffraction-limited beam quality have been limited to below 50 mJ and at modest average output powers [20]. Relevant high average power results, summarised in Table 1, are all room-temperature laser geometries, generating pulses at ~ 2 µm using either multiple pump sources or gain media, resulting in either poor beam quality and slope efficiency and/or complex laser systems.

Cryogenic cooling offers vast improvements in thermo-optical and thermo-mechanical properties of quasi three-level gain media, but only low average power has been achieved [21]. One of the key benefits from cryogenic cooling comes from the reduction of the thermal population of the lower lasing level, resulting in a four-level like behaviour. This significantly reduces the pump power required to achieve transparency and allows for much larger mode volumes to be used when compared to room-temperature operation of such lasers [21]. The benefit of cryogenic cooling was

✉ Miftar Ganija
miftar.ganija@dst.defence.gov.au; miftaganija@gmail.com

[1] Department of Physics and IPAS, The University of Adelaide, Adelaide, SA 5005, Australia

[2] Directed Energy Technologies and Effects, Weapons and Combat Systems Division, DST Group, Edinburgh, SA 5111, Australia

Table 1 Summary of known Q-switched lasers, at 2 µm, with average power > 10 W, energy per pulse > 20 mJ and $M^2 < 1.5$, all at room temperature. Previously no cryogenic lasers satisfied simultaneously these requirements

Number and type of gain crystals	Pulse energy (mJ)	PRF at high energy	Average power under pulsed operation (W)	Reference
3 × Ho:YLF	170	500 Hz	86	Dergachev et al. [17]
3 × Ho:YLF	330	50 Hz	16.5	Strauss et al. [18]
3 × Ho:YAG	23.1	10 kHz	231	Ben-Rui Zhaog et al. [19]

demonstrated as early as 1980, with Ho^{3+} in YAG and YLF, flashlamp pumped in a co-doped laser [22]. More recently, high-energy operation of a pulsed Ho:YLF laser at cryogenic temperatures were reported by Fonnum et. al [23], in which pulse energies up to 550 mJ were produced at a 1 Hz pulse repetition frequency (PRF), with the authors reporting limitations at higher average output powers, as well as associated beam quality degradation. Thus, the high energy scaling of the cryogenic Ho^{3+} in YAG host is yet to be demonstrated.

The lack of progress has been attributed partly to the lack of available, narrow linewidth, pump sources at 1.9 µm. The stringent requirements on the pump sources are due to the narrow absorption linewidth of cryogenic Ho:YAG [24–26] and to the complexity associated with assembling a laser head at room temperature and subjecting it to cryogenic cooling. In previous work of the authors, they have successfully addressed both these issues and reported a scalable high-power laser approach, which used a laser crystal mounted in a carefully engineered molybdenum housing, providing conduction cooling and repeated cryogenic cycling as described in detail in [27, 28].

In this paper, we report, to the best of our knowledge, the first cryogenically cooled Q-switched Ho:YAG oscillator, resonantly pumped by a thulium fibre laser operating at 1907 nm, including average power and energy scaling. The results obtained have significantly advanced the field by achieving a combination of higher average power and higher energy per pulse at higher PRFs using a simple laser oscillator.

2 Laser configuration

A schematic of the cryogenically cooled Ho:YAG is shown in Fig. 1. The Ho:YAG crystal was 3 × 2 × 50 mm and doped at 0.5 at%. It was mounted in their configuration as described in [27, 28]. The cryostat windows were AR coated CaF_2 with a transmission of 98.5% at both the pump and laser wavelengths. The V-shaped laser resonator was formed using a highly reflective flat dichroic mirror (D_1) at ~ 45° with high transmission at 1907 nm and high reflectivity at 2097 nm.

The spectral widths of the Ho:YAG absorption lines in the 1905–1911 nm region are approximately 0.3 nm at cryogenic temperatures [21], which compares favourably with the < 0.15 nm linewidth of the high-power TDFLs used [29]. Both the 1907 nm and 1908 nm absorption strengths are high and not influenced by atmospheric water absorption. Here, they only focus on the laser performance when pumped by a 1907 nm TDFL, but they also obtained very similar results when pumping at 1908 nm in CW operation [28]. The pump laser was measured to have a diffraction limited beam quality ($M^2 < 1.05$) and excellent pointing stability at all operating powers. The wavelength of the laser was defined by fibre Bragg gratings (FBG) [29] and was accurately tuned by controlling the temperature of the FBG's in the laser cavity. The TDFL was terminated using a slightly angled, bulk 10 × 10 × 10 mm, anti-reflection (AR)-coated Infrasil endcap attached using CO_2 laser processing. The bulk endcap reduced back-reflections into the laser cavity and simplified the mounting and collimation of the fibre laser output. The pump beam was focused by an aplanatic lens ($f = 25$ mm) and launched into the gain medium through D_1. A small portion of the pump light experienced a residual reflection from D_1 and was coupled into an optical spectrum analyzer (OSA).

Similarly, the leakage of Ho:YAG intracavity laser signal from D_1 was also coupled into the OSA. This enabled the pump and laser wavelengths to be monitored simultaneously. Another dichroic in the output beam of the laser, D_2, was used to separate any transmitted pump from the laser output. The schematic includes the vacuum envelope of the cryostat, the windows through which the pump and laser beams pass and the laser resonator formed by mirrors M_1 and M_2. M_1 was a concave mirror with a radius of curvature of 1000 mm, coated for high reflectivity (HR) at the lasing wavelength of 2097 nm. M_2 was the output coupler formed by a combination of a flat 30% reflectivity mirror immediately adjacent to an AR-coated lens with a focal length of 750 mm, this combination effectively acting as a curved mirror, reflectivity 30% and radius of curvature of 750 mm. The resonator mirrors were separated by 1600 mm in a near confocal resonator with a waist at the centre of the Ho:YAG slab. The $1/e^2$ mode diameters of the pump and lasing modes were optimised to be ~ 1.2 mm and ~ 1.1 mm, respectively.

The Q-switch consisted of a quarter-wave rubidium titanyl phosphate (RTP) Pockels cell and a quarter-wave plate

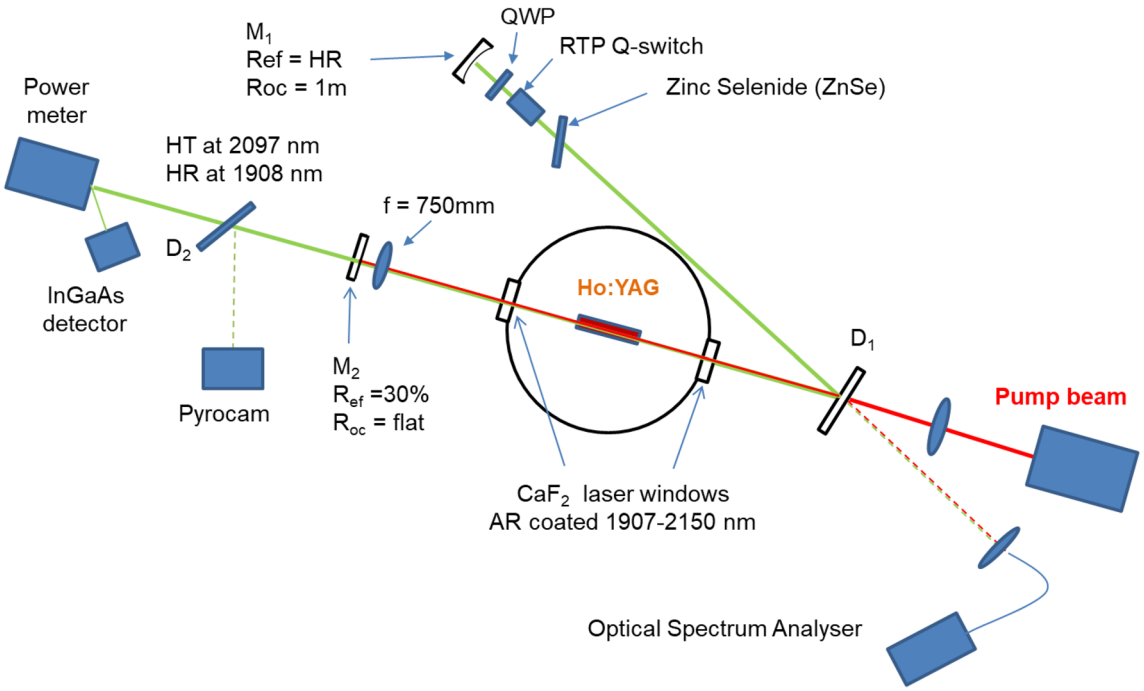

Fig. 1 Schematic of the optical layout of the Q-switched cryogenically cooled Ho:YAG laser, including the Q-switch elements: ZnSe polariser, RTP Q-switch, quarter-wave plate, extended InGaAs detector, external pump laser optics and the diagnostics used. The red lines represent the pump beam path and the green lines represent the lasing beam path

(QWP), with a ZnSe plate at Brewester angle acting as a polariser to provide hold-off.

Pulsed operation was characterised at different pump powers and pulse repetition rates (PRFs) ranging from 200 to 1000 Hz. The beam quality of the laser was determined by focusing the output beam and measuring the beam profile as a function of distance as described below.

3 Experimental results

The laser was initially operated as continuous wave (CW) with no Q-switch elements inserted. As shown in Fig. 2, the laser produced output power > 52 W with a slope efficiency of 72% measured with respect to the launched pump power. With the Q-switching elements inserted into the cavity, but still operating CW, the slope efficiency reduced to 70%. The QWP was then rotated to prevent CW operation and the Q-switched was triggered at PRFs of 1 and 2 kHz producing output energies in the 25–50 mJ per pulse range.

The highest average powers observed in Q-switched operation was 52 W for PRF = 2 kHz, which consisted of 26 mJ pulses, and 51 W for PRF = 1 kHz, which consisted of 51 mJ pulses. Decreasing the PRF at constant pump power increased the pulse energy and decreased its duration, as expected. The linear proportionality of the average output power to the CW pump power shows that the laser was not limited by thermal effects in the gain medium, the output power being limited only by the pump power available.

The pulse duration vs pulse energy for a range of average output powers from 1 to 33 W controlled by the pump power was recorded. The pulse duration vs output energy for different average powers due to different pump powers is shown in Fig. 3. The pump power was kept constant for each run and the pulse shape narrowed from ~ 250 to 90 ns as the PRF was lowered and the energy per pulse increased. Since the launched pump power for each curve was stable, the average output power was monitored while changing the PRF from 1000 Hz down to 200 Hz. Also shown are two curves with average powers of 51 W and 52 W at fixed PRFs of 1 kHz and 2 kHz, respectively. In these cases, the PRF was fixed and the pump power changed to vary the output power. The consistency of the pulse durations at higher pulse energies, independent of average laser power and PRF, demonstrates excellent thermal behaviour of the gain media at cryogenic temperature, an essential requirement for further scaling. Also note that the constant monitoring of the power at the ZnSe plate showed no power increase even when operating at maximum pulse energies 165 mJ. The slope efficiency of the laser did not reduce below 62% with respect to the launched pump power as shown in Fig. 2.

The maximum average power measured was 33 W, at a PRF of 200 Hz corresponding to 165 mJ with 90 ns pulse duration.

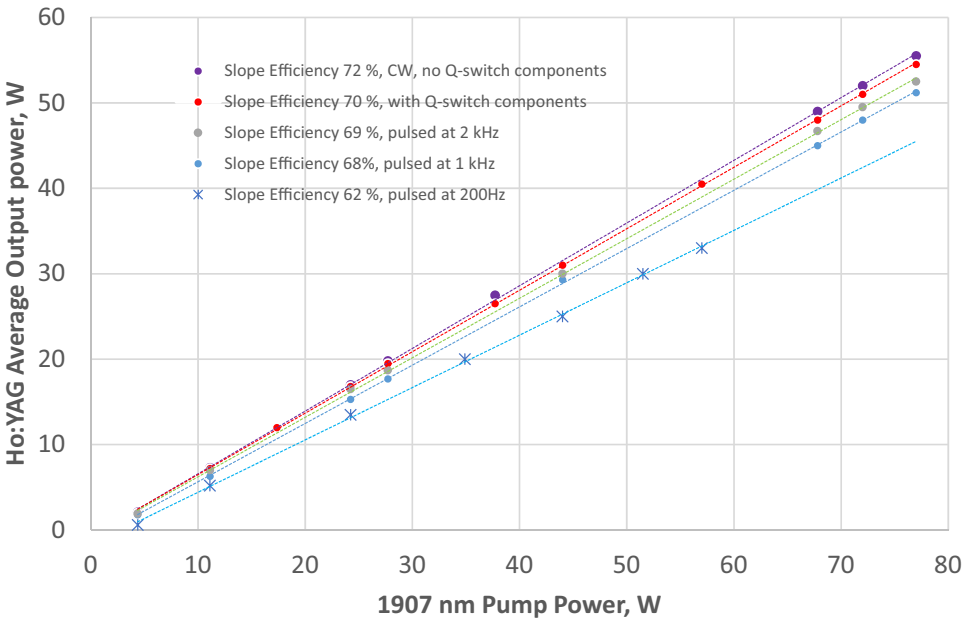

Fig. 2 Average output power of the Ho:YAG laser at 2098 nm as a function of 1907 nm pump power for various lasing conditions, including CW lasing with and without Q-switch components and Q-switched lasing at several PRFs

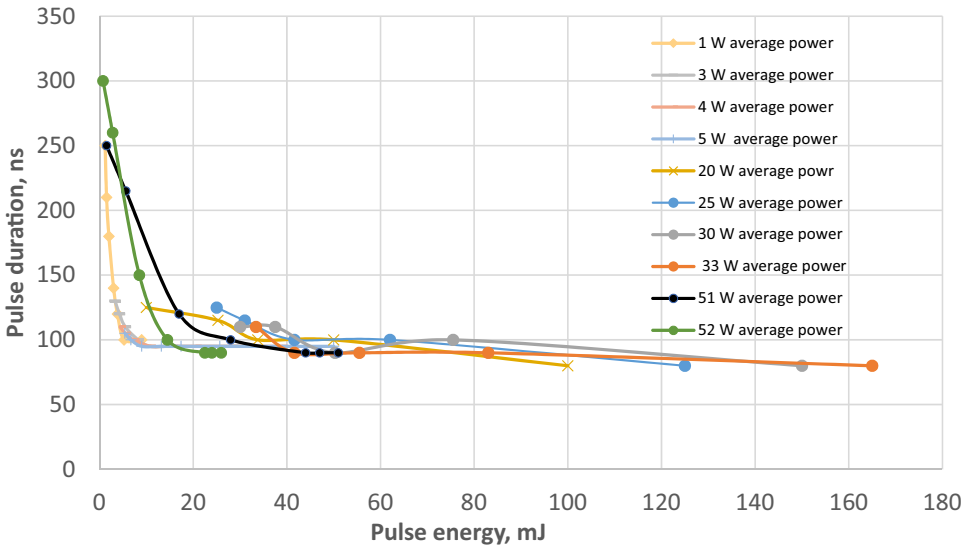

Fig. 3 The pulse width of the Q-switched cryogenic laser dependent on the pulse energy and is independent of average power. Average powers range from 1 to 33 W, PRFs from 200 to 1000 Hz and the pulse width measured as full width at half maximum (FWHM). Also shown are two additional sets of data at 51 and 52 W (see text)

The laser beam quality exhibited no degradation even at the higher power levels and pulse energies. However, in order to avoid possible damage to the coatings, the detailed laser performance measurements including beam quality was measured at lower pulse energies.

A typical example of the temporal pulse shape at 135 mJ per pulse at 200 Hz is shown in Fig. 4a. The spectrum of the laser output was centred at 2097.5 nm with a FWHM of 0.2 nm as shown in Fig. 4b.

The average beam quality of the pulsed laser was determined by focussing a small percentage (0.5%) of a large number of pulses of the output beam onto a pyro camera and the average beam profile measured as a function of distance through the focus by moving the camera on a calibrated track. In the region close to focus, the beam spot size approached the size of a single camera pixel, and a magnifying imaging system (5 × transverse magnification) was used to provide meaningful, resolved beam profiles. Figure 5 shows the beam quality measurement with the laser operating at 135 mJ pulse energy and a 200 Hz repetition rate with $M^2 < 1.14$.

The beam quality at the maximum power and energy was observed qualitatively in near and far field to be indistinguishable from those where detailed measurements were made. In general, the beam quality was unaffected by the average power, PRF and single pulse energy, thus showing the potential for further scaling with increased pump power.

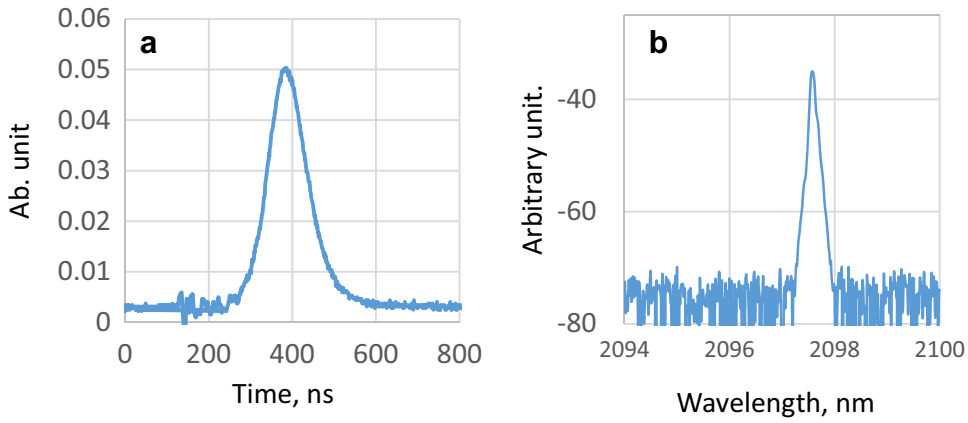

Fig. 4 **a** Oscilloscope trace of the 135 mJ pulse at 200 Hz PRF and **b** the corresponding emission line of the Ho:YAG laser measured with a resolution setting of 0.05 nm

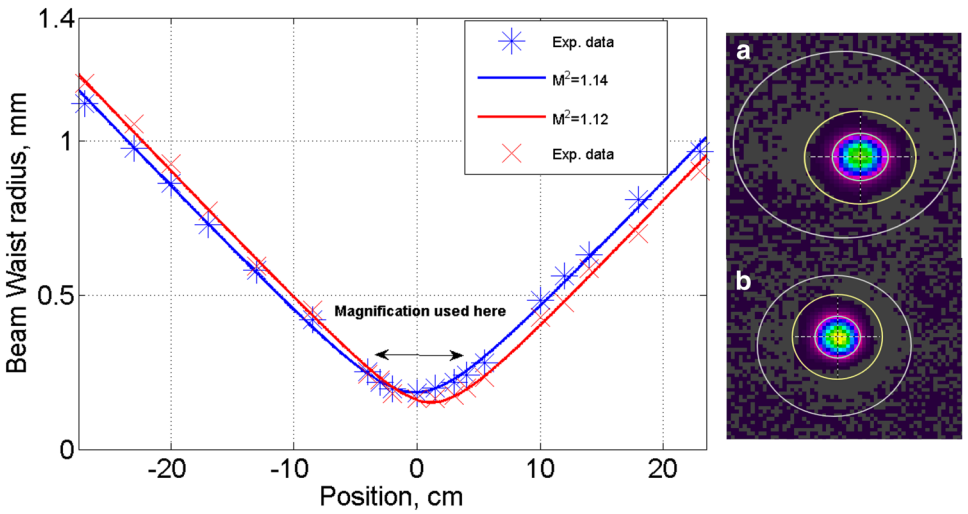

Fig. 5 Beam radius measurements through the focus of the laser beam at 27 W average output at 200 Hz. The lines of best fit correspond to an $M^2_{X,Y} = 1.14, 1.12$. **a** Near-field profile of the laser at 27 W average power. **b** Far-field profile of the Ho:YAG laser average output at 27 W viewed with an imaging system with a magnification of 5.0X (FWHM)

4 Discussion

The authors have investigated and characterised a Q-switched Ho:YAG laser under cryogenic conditions. The increased absorption coefficient due to cryogenic conditions enabled the efficient absorption of the pump radiation even with a relatively short and low-doped crystal (50 mm, 0.5 at.%). As reported previously [21], the reduced threshold allowed for the operation with relatively large mode diameter (1.1 mm). These two scaling features are of significant interest for further energy and power scaling of Ho:YAG gain media.

A consistent reduction in the average power was observed as the PRF was reduced below 200 Hz. Since there was no thermal distortion or increased losses even at high power, this behaviour is ascribed to the period between pulses approaching the upper state lifetime. However, further investigations are required to quantify this effect.

In this work, high energy pulses at lower repetition frequencies have been demonstrated at 2.1 µm. As pointed out in the introduction prior work published has shown impressive results at low repetition rates. However, there are number of applications that benefit from high energy pulses at higher PRFs. The major challenge in the path to achieve such high energy pulses is the avoidance of damage to the laser resonator components due to high peak power densities.

5 Conclusion

This work demonstrates the benefits of cryogenic cooling for Q-switched operation of Ho:YAG; it enables low threshold, avoids a high pump power requirement and uses low doping concentrations. This reduces the number of pump lasers and gain crystals required to achieve output energies of > 20 mJ, while still enabling average power scaling. The laser damage threshold requires further investigation for possible high-energy pulse operations.

This work presents the first Q-switched cryogenically cooled, resonantly pumped high-pulse energy Ho:YAG laser. Compared to the approaches summarised in Table 1, this work also represents a significant reduction in complexity

and a significant scaling of energy. These results also show the clear advantage of high-energy per pulse operation of Ho:YAG at cryogenic conditions. The system shows no degradation due to thermal issues suggesting that higher pulse energies could be achieved in the future utilizing a larger cavity mode area as well as an amplifier configuration.

Acknowledgements The authors gratefully acknowledge support from The University of Adelaide Fellowship Scheme and excellent support from the physics workshop at The University of Adelaide.

References

1. P. Budni, L. Pomeranz, M. Lemons, C. Miller, J. Mosto, E. Chicklis, J. Opt. Soc. Am. B **17**, 723 (2000)
2. D. Creeden, P.A. Ketteridge, P.A. Budni, S.D. Setzler, Y.E. Young, J.C. McCarthy, K. Zawilski, P.G. Schunemann, T.M. Pollak, E.P. Chicklis, M. Jiang, Opt. Lett. **33**, 315 (2008)
3. E. Lippert, H. Fonnum, G. Arisholm, K. Stenersen, Opt. Express **18**, 26475 (2010)
4. A. Hemming, J. Richards, A. Davidson, N. Carmody, S. Bennetts, N. Simakov, J. Haub, Opt. Express **21**, 10062–10069 (2013)
5. B.-Q. Yao, Y.-J. Shen, X.-M. Duan, T.-Y. Dai, Y.-L. Ju, Y.-Z. Wang, Opt. Lett. **39**, 6589 (2014)
6. M. Eichhorn, M. Schellhorn, M.W. Haakestad, H. Fonnum, E. Lippert, Opt. Lett. **41**, 2596 (2016)
7. O. Chalus, P. Schunemann, K. Zawilski, J. Biegert, M. Ebrahim-Zadeh, Opt. Lett. **35**, 4142 (2010)
8. G. Marchev, A. Tyazhev, V. Petrov, P.G. Schunemann, K.T. Zawilski, G. Stöppler, M. Eichhorn, Opt. Lett. **37**, 740 (2012)
9. B. Cole, L. Goldberg, S. Chinn, L.A. Pomeranz, K.T. Zawilski, P.G. Schunemann, J. McCarthy, Opt. Lett. **43**, 1099–1102 (2018)
10. Y.J. Shen, B.Q. Yao, X.M. Duan, G.L. Zhu, W. Wang, Y.L. Ju, Y.Z. Wang, Opt. Lett. **37**, 3558–3560 (2012)
11. A. Hemming, J. Richards, S. Bennetts, A. Davidson, N. Carmody, P. Davies, L. Corena, D. Lancaster, Opt. Commun. **283**, 4041–4045 (2010)
12. L. Wang, X. Cai, J. Yang, X. Wu, H. Jiang, J. Wang, Opt. Lett. **37**, 1986 (2012)
13. J. Yu, B.C. Trieu, E.A. Modlin, U.N. Singh, M.J. Kavaya, S. Chen, Y. Bai, P.J. Petzar, M. Petros, Opt. Lett. **31**, 462 (2006)
14. Yu Jirong, A. Braud, M. Petros, Opt. Lett. **28**, 540–542 (2003)
15. S. Lamrini, P. Koopmann, M. Schafer, K. Scholle, P. Fuhrberg, Appl. Phys. B **106**, 315–319 (2012)
16. K. Scholle, P Fuhrberg P (2008) In-band pumping of high-power Ho:YAG lasers by laser diodes at 1.9 μm, in *Conference on Lasers and Electro-Optics* (San Jose, CA, 4–9 May 2008) (Optical Society of America) paper CTuAA1.
17. A. Dergachev, D. Armstrong, A. Smith, T. Drake, M. Dubois, Proc. SPIE **6875**, 687507 (2008)
18. H.J. Strauss, D. Preussler, M.J.D. Esser, W. Koen, C. Jacobs, O.J.P. Collett, C. Bollig, Opt. Lett. **38**, 1022–1024 (2013)
19. B.-R. Zhao, B.-Q. Yao, C.-P. Qian, G.-Y. Liu, Yi Chen, R.-X. Wang, T.-Y. Dai, X.-M. Duan, Opt. Lett. **43**, 5989–5992 (2018)
20. P.A. Budni, C.R. Ibach, S.D. Setzler, E.J. Gustafson, R.T. Castro, E.P. Chicklis, Opt. Lett. **28**, 1016–1018 (2003)
21. M. Ganija, N. Simakov, A. Hemming, J. Haub, P. Veitch, J. Munch, Opt Express **24**, 11569–11577 (2016)
22. N.P. Barnes, D.J. Gettemy, IEEE J Quantum Electron. **17**, 1303 (1981)
23. H. Fonnum, E. Lippert, M.W. Haakestad, Opt. Lett. **38**, 1884–1886 (2013)
24. J.I. Mackenzie, J.W. Kim, L. Pearson, W.O.S. Bailey, Y. Yang, W.A. Clarkson, Proc. SPIE **7578**, 75781F (2010)
25. D.C. Brown, V. Envid, J. Zembek, Appl. Opt. **51**, 8147–8158 (2012)
26. M. Ganija, N. Simakov, A. Hemming, J. Haub, P. J. Veitch, J. Munch, in *Conference on Lasers and Electro-Optics*, OSA Technical Digest (2016) (Optical Society of America, 2016), paper STu4M.3.
27. M. Ganija, D. Ottaway, P. Veitch, J. Munch, Opt. Express **21**, 6973–6978 (2013)
28. M. Ganija, A. Hemming, N. Simakov, K. Boyd, J. Haub, P. Veitch, J. Munch, Opt. Express **25**, 31889–31895 (2017)
29. N. Simakov, A.V. Hemming, A. Carter, K. Farley, A. Davidson, N. Carmody, M. Hughes, J.M.O. Daniel, L. Corena, D. Stepanov, J. Haub, Opt. Express **23**, 3126–3133 (2015)

Publisher's Note Springer Nature remains neutral with regard to jurisdictional claims in published maps and institutional affiliations.